Transactions, SMiRT-25
Charlotte, NC, USA, August 4-9, 2019
Division V – Modelling, Testing and Response Analysis of Structures, Systems and Components

EFFECTS OF MECHANICAL PROPERTIES OF LRB ON SEISMIC PERFORMANCE OF BASE-ISOLATED NPP STRUCTURES

Duy-Duan Nguyen[1], Bidhek Thusa[2], Hyosang Park[3], Hoyeop Lee[4], and Tae-Hyung Lee[3]

[1] Postdoctoral Researcher, Department of Civil and Environmental Engineering, Konkuk University, Seoul, Korea (duyduan@konkuk.ac.kr)
[2] MS Student, Department of Civil and Environmental Engineering, Konkuk University, Seoul, Korea
[3] Postdoctoral Researcher, Department of Civil and Environmental Engineering, Konkuk University, Seoul, Korea
[4] Postdoctoral Researcher, Department of Civil and Environmental Engineering, Konkuk University, Seoul, Korea
[5] Professor, Department of Civil and Environmental Engineering, Konkuk University, Seoul, Korea

ABSTRACT

A base isolation system plays an important role for improving the seismic performance of infrastructures including nuclear power plants (NPPs). The lead rubber bearing (LRB) is one of the most widely used base isolation bearings for civil and NPP structures. The purpose of this study is to investigate the effect of the mechanical properties of LRB on seismic performance and fragility of base-isolated NPP structures. Three mechanical properties of LRB, namely elastic stiffness, yield strength, and hardening ratio, are assumed as the most influential properties and considered in numerical analyses. The floor response spectra (FRS) of the containment building are calculated for all the cases of changing LRB properties. In addition, the fragility curves are developed for various limit states, which are defined based on the shear deformation of LRB. The numerical results reveal that the FRS was significantly changed with a variation of the elastic stiffness of LRB. In contrast, the variation of the hardening ratio of LRB did not affect FRS of RCB. A variation of the yield strength of LRB moderately changes FRS of RCB. Moreover, the effects of various properties of LRB on seismic fragility curves of the NPP are shown to be trivial.

INTRODUCTION

A damage of nuclear power plant (NPP) can give catastrophes to humans and environment. There were some nuclear accidents caused by strong earthquakes in recent time, typically the radioactive releases due to the 2011 Tohoku (Japan) earthquake. The study on seismic performances and evaluations of NPP structures are always important and needed.

A base isolator such as lead rubber bearing (LRB) or friction pendulum system can mitigate the possibility of damage to the civil structures and NPPs during an earthquake. The effect of mechanical properties of LRB on seismic performance of infrastructures was studied numerously (Hameed et al., 2008; Lee and Nguyen, 2018; Kim et al., 2019; Providakis, 2008). For NPP structures, there were few studies conducted the influence of LRB properties on seismic responses of such structures. Jung et al. (2017) investigated the effect of second hardening of Bouc-Wen model for LRB on floor response spectra of base-isolated NPP. Choun et al. (2014) evaluated the effects of variability of the properties of LRB including material variability in manufacturing, aging, and operation temperature on responses of a base-isolated NPP structure. Cho et al. (2015) analyzed the vertical seismic responses of based-isolated NPP structures using LRBs. Lee and Song (2015) compared the seismic responses of seismically isolated NPP containment

structures using equivalent linear- and nonlinear-lead-rubber bearing models. However, the aforementioned works did not sufficiently investigate effects of elastic stiffness, yield strength, and hardening ratio of LRB on floor response spectra and fragility curves of NPP structures.

This study performs a series of time history analysis to evaluate the effects of mechanical properties of LRB on responses of NPP structures. Elastic stiffness, yield strength, and hardening ratio are selected as possible influential properties of LRB and considered in numerical analyses. Seismic responses of the based-isolated NPP structures are focused on floor response spectra (FRS) and shear deformation of LRB. Thereafter, a set of fragility curves for different limit states, which are defined based on shear strain capacity of LRB, is developed. Finally, the influence of LRB properties on seismic performances of NPP structures is discussed.

NUMERICAL MODELING

A base-isolated APR1400, a recently developed nuclear reactor type in Korea, is employed for a numerical example in this study. The lumped mass stick model of NPP is developed in SAP2000, as shown in Figure 1. Three structural components, which are reactor containment building, internal structure, and auxiliary structure, are modelled using so-called lumped-mass stick model. All structures share with a base mat that is modelled in terms of rigid shell elements. In order to improve the seismic performance of the structure, 468 lead rubber bearings are installed beneath the base mat. A bilinear behaviour model is assigned to all LRBs, as shown in Figure 2.

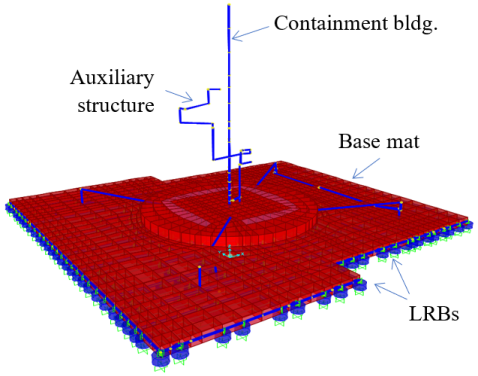

Figure 1. Lumped mass stick model of NPP

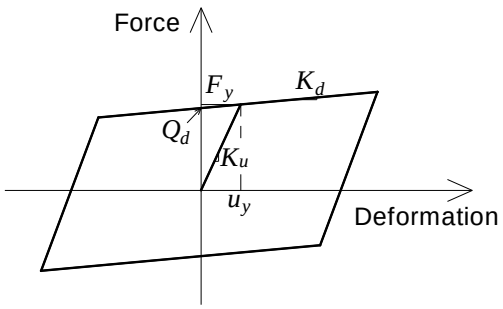

Figure 2. Bilinear behaviour model of LRB

The variations of LRB properties including the elastic stiffness (K_u), yield strength (F_y), and hardening ratio (K_d/K_u, K_d is the post yield stiffness) considered in this study are illustrated in Figure 3. Tables 1-3 contain the mechanical properties of LRB with the variation of elastic stiffness, yield strength,

and hardening ratio, respectively. Three different levels of the elastic stiffness of LRB are considered and referred to as LRB-Ku1, LRB-Ku2, and LRB-Ku3. Similarly, for the variation of yield strength, it is referred to as LRB-Fy1, LRB-Fy2, and LRB-Fy3. Likewise, LRB-Kd1, LRB-Kd2, and LRB-Kd3 are referred to the variation of hardening ratio.

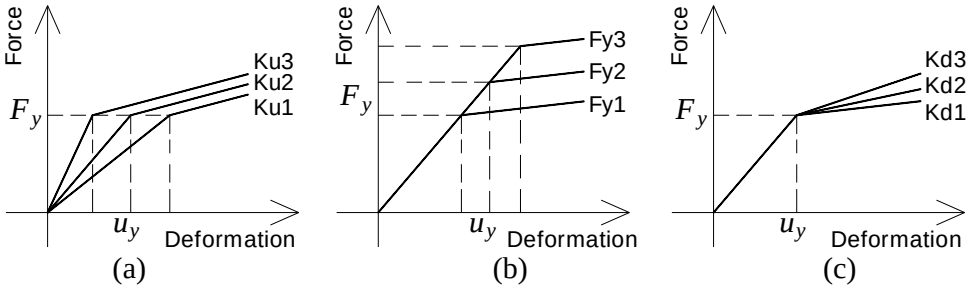

Figure 3. Various LRB properties: (a) elastic stiffness, (b) yield strength, and (c) hardening ratio

Table 1: Mechanical properties of LRBs with various elastic stiffness.

Parameter	LRB-Ku1	LRB-Ku2	LRB-Ku3
Elastic stiffness, K_u, (kN/m)	322,622	537,703	806,555
Post yield stiffness, K_d, (kN/m)	5,377	5,377	5,377
Effective stiffness, K_e, (kN/m)	6,794	8,945	11,633
Yield strength, F_y, (kN)	1,009	1,009	1,009

Table 2: Mechanical properties of LRBs with various yield strength.

Parameter	LRB-Fy1	LRB-Fy2	LRB-Fy3
Elastic stiffness, K_u, (kN/m)	537,703	537,703	537,703
Post yield stiffness, K_d, (kN/m)	5,377	5,377	5,377
Effective stiffness, K_e, (kN/m)	8,321	8,945	9,658
Yield strength, F_y, (kN)	807	1,009	1,211

Table 3: Mechanical properties of LRBs with various hardening ratio.

Parameter	LRB-Kd1	LRB-Kd2	LRB-Kd3
Elastic stiffness, K_u, (kN/m)	537,703	537,703	537,703
Post yield stiffness, K_d, (kN/m)	3,764	5,377	8,066
Effective stiffness, K_e, (kN/m)	7,342	8,945	11,615
Yield strength, F_y, (kN)	1,009	1,009	1,009

SEISMIC RESPONSE OF BASE-ISOLATED NPP STRUCTURES

We perform a series of time-history analyses in the horizontal direction to obtain the seismic responses of the base-isolated NPP model. A set of 24 ground motion records including recent Korean earthquakes is selected for dynamic analyses. The superstructures are assumed to behave in an elastic range during a design earthquake due to an energy-absorbing behaviour of the base isolators. It is important to note that the secondary systems (e.g. cabinets, relays) are attached to the primary structures at the floors or walls, so that their responses are predominantly affected by the motions at floors/walls where they are attached (Park et al., 2017; Xie et al., 2019). Therefore, in this study, the seismic responses of the base-isolated NPP structures are monitored in terms of floor response spectra of RCB and the shear deformation of LRB.

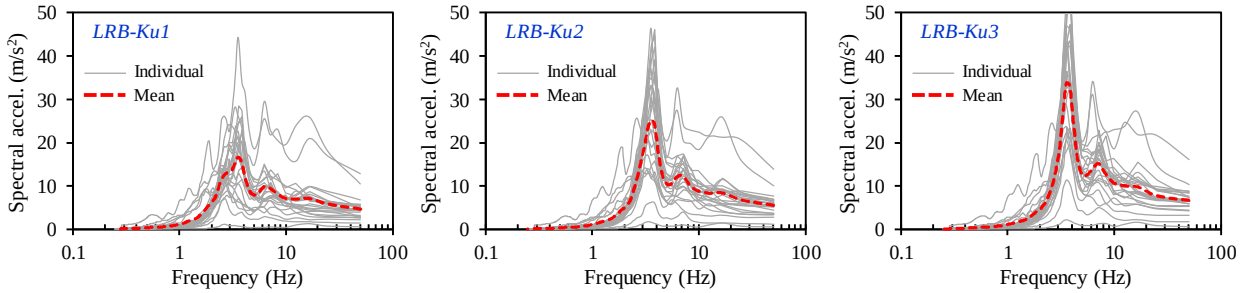

(a) FRS at the top of RCB for various elastic stiffness of LRB

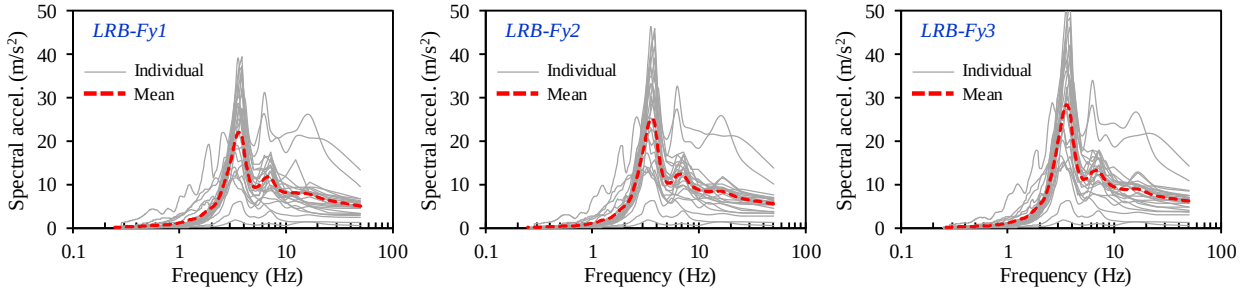

(b) FRS at the top of RCB for various yield strength of LRB

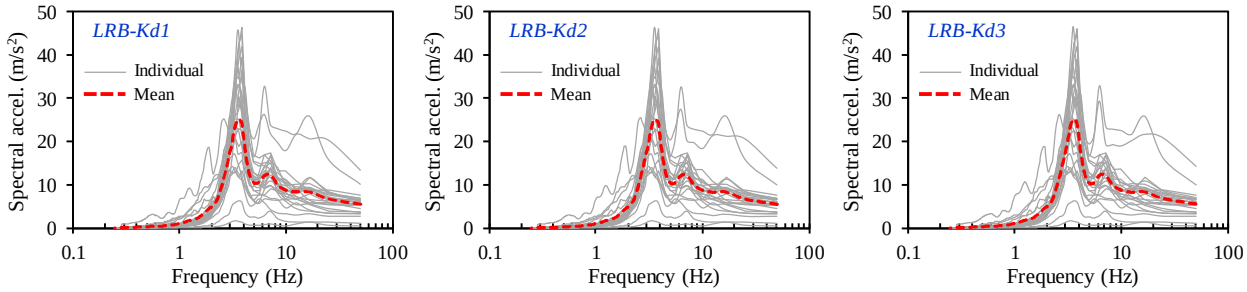

(c) FRS at the top of RCB for various hardening ratio of LRB

Figure 4. FRS at the top of RCB during unscaled motions (PGA_{mean} = 0.24g)

Figure 4 shows the FRS at the top of RCB considering the variation of elastic stiffness, yield strength, and hardening ratio of LRB. The floor responses are amplified and reach the maxima at frequency of approximately 3.84 Hz (i.e. the dominant frequency of RCB) for all the cases. It can be observed that the FRS is significantly increased with the increment of elastic stiffness of LRB. Particularly, at the dominant frequency of RCB (3.84 Hz), FRS of LRB-Ku3 is about 2.1 times larger than that of LRB-Ku1. Meanwhile, FRS of LRB-Fy3 is about 1.2 times larger than that of LRB-Fy1 at 3.84 Hz. The FRS is not affected by

changing hardening ratio of LRB. This can be attributed to the reason that an increment of LRB stiffness causes to reduce the hysteretic energy, therefore, the inertia force at structural floors and floor accelerations are increased. Likewise, the hysteretic energy of LRB is decreased since its yield strength increases. Moreover, the change of hardening ratio trivially changes the hysteretic energy of LRB.

Figure 5 shows FRS at the top of RCB accounting for variations of the elastic stiffness, yield strength, and hardening ratio of LRB due to ground motions scaled to PGA 1.0g. FRS is slightly increased as the elastic stiffness and yield strength of LRB increases by approximately by 20% at the frequency of 3.84 Hz. The FRS is not also affected by changing of the hardening ratio of LRB. Moreover, a large amplification of FRS distributes in a wider band of frequency, from 3 Hz up to 10 Hz. It indicates the electrical devices and equipment (e.g. relay cabinet, generator control panel, switch gear, motor control centre, and instrument panel), which own a fundamental frequency from 5-10 Hz, might be vulnerable to a large earthquake.

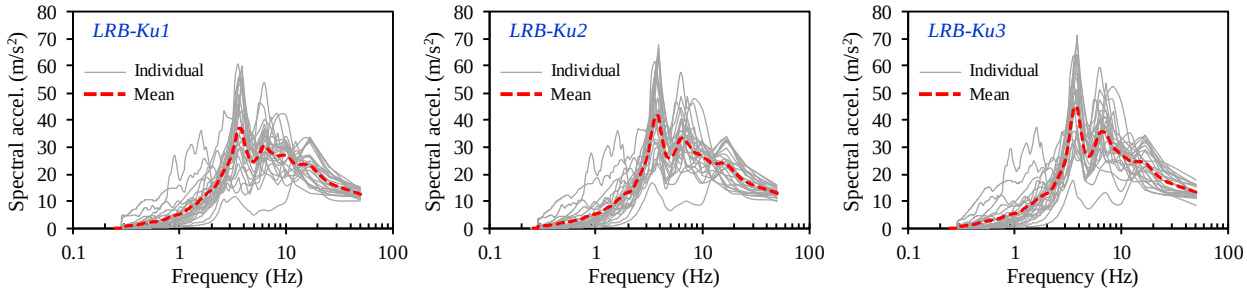

(a) FRS at the top of RCB for various elastic stiffness of LRB

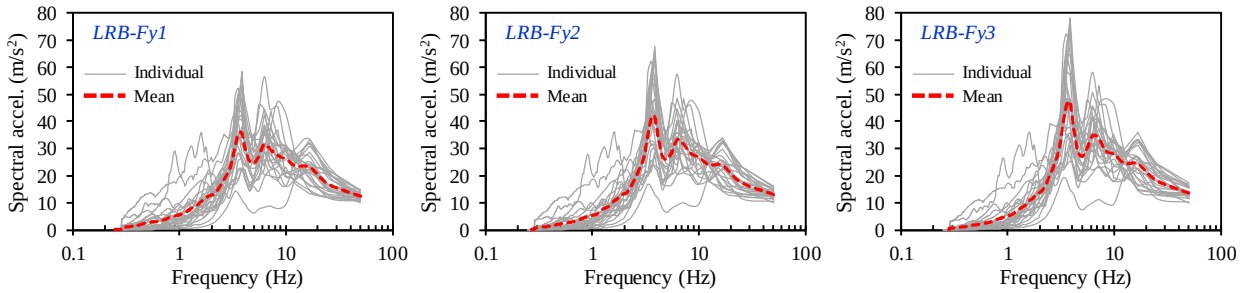

(b) FRS at the top of RCB for various yield strength of LRB

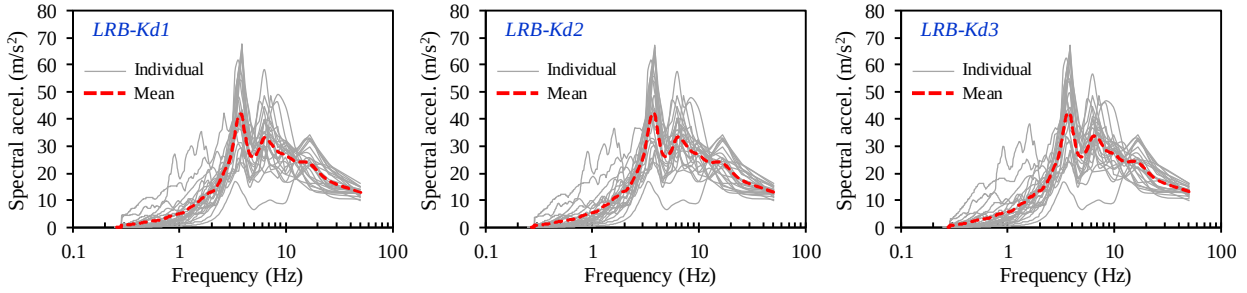

(c) FRS at the top of RCB for various hardening ratio of LRB

Figure 5. FRS at the top of RCB during ground motions scaled to PGA = 1.0g

Figure 6 shows the comparison of FRS with various levels of PGA of ground motions. FRS of the containment structure is increased as the level of PGA of ground motions increased. In addition, the high spectral acceleration band on the spectrum curve is widened to the higher frequency region with an

increment of PGA. This is again to emphasize that the electrical devices can be affected by ground motions with a high amplitude.

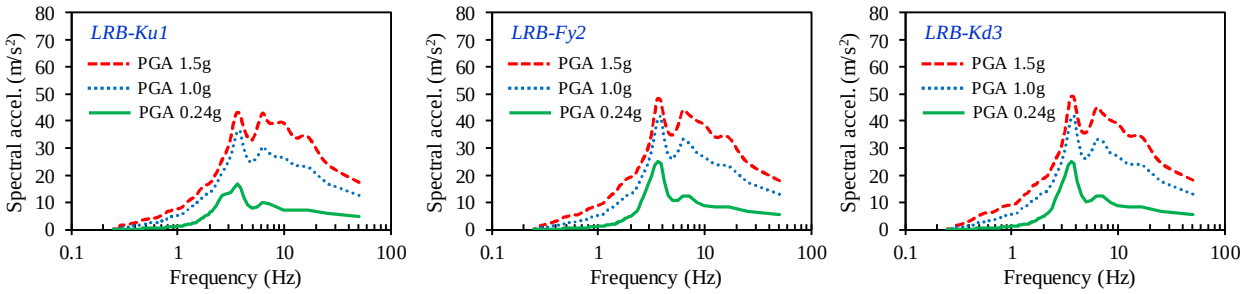

Figure 6. Comparison of FRS in various PGA levels of ground motions

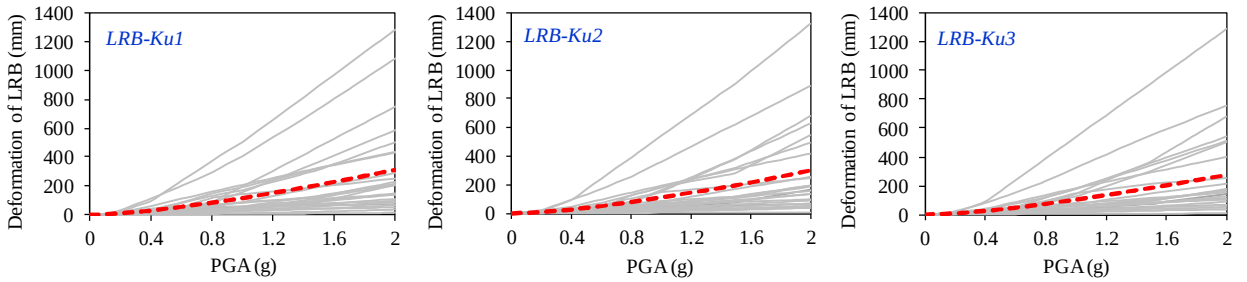

(a) Variation of elastic stiffness

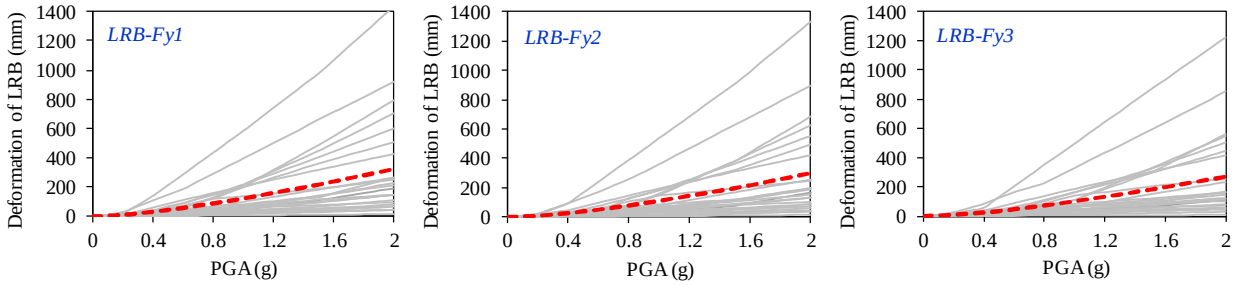

(b) Variation of yield strength

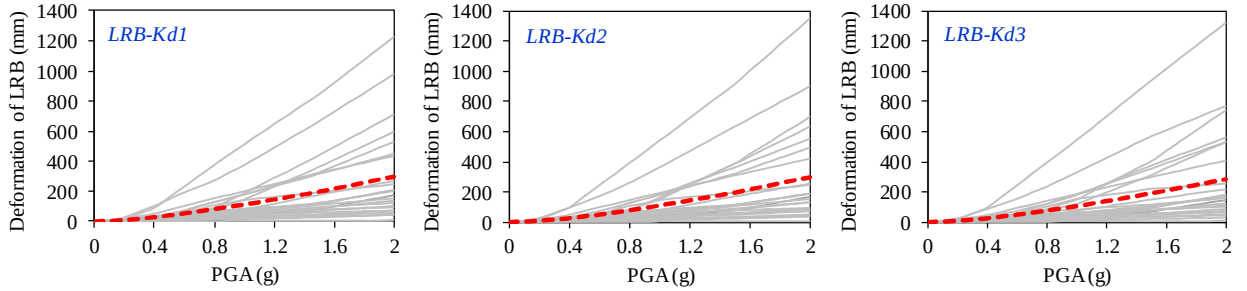

(c) Variation of hardening ratio

Figure 7. Incremental displacement of LRB with respect to PGA

Since LRB is the crucial element in base-isolated NPP structures, we pay attention to the nonlinear response of this member in terms of shear deformation. The aforesaid motion suite is utilized to perform

the incremental dynamic analysis (IDA). In IDA, each ground motion is scaled to multiple levels of intensity. Here, we select PGA as an intensity measure of earthquakes. For each analysis, the maximum deformation of LRB is monitored as the engineering demand parameter. In total, 4320 dynamic analyses were performed (i.e. 9 LRB cases x 24 records x 20 intensity levels).

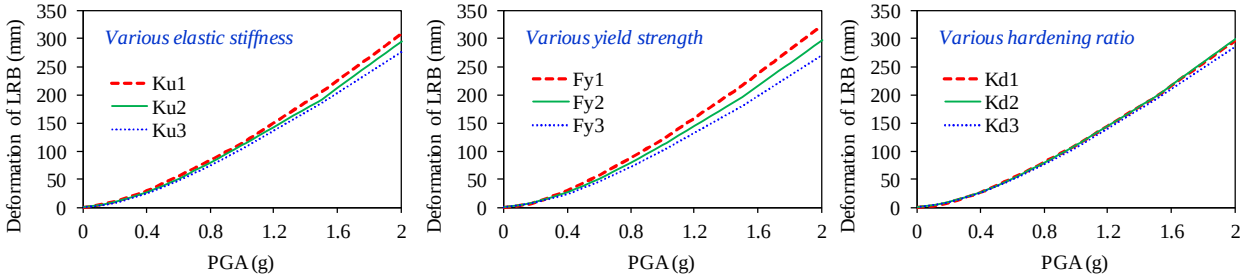

Figure 8. Comparison of deformations in various properties of LRB

Figures 7 shows the IDA curves in terms of the deformation of LRB versus PGA for various mechanical properties of LRB. The dashed solid curves represent the mean values. It is obvious to observe that the shear deformation of LRB is increased together with an increment of PGA. Figure 8 shows the comparison of deformations of LRB with various properties of LRB. The deformation of LRB is gradually reduced as the elastic stiffness and yield strength of LRB increased. Meanwhile, the change of hardening ratio parameter does not affect the deformation of LRB, even in a higher PGA.

FRAGILITY CURVE

In order to derive fragility curves, a set of limit states, which represents damage levels of structural components, should be defined. In this study, we defined three limit states, namely slight, moderate, and extensive based on the shear strain of LRB. The shear strain is expressed by the ratio of the maximum lateral deformation (Δ) and the height of LRB (H). Based on previous studies (Eem and Hahm, 2019; Kim et al., 2016; Yabana et al., 2009), LRB may be broken around 500% shear strain. Therefore, we adopted these results to define three limit states. If the shear strain exceeds 100% (i.e. $\Delta \geq 224$ mm), the slight limit state (LS-1) is established. Similarly, if the shear strain reaches 300% (i.e. $\Delta \geq 672$ mm) and 400% (i.e. $\Delta \geq 896$ mm), the moderate (LS-2) and extensive (LS-3) limit states are specified, respectively. This approach was also applied in studies elsewhere (Ali et al., 2014; Lee and Song, 2015; Nguyen et al. 2018, 2019; Zhang and Huo, 2008).

A fragility function expresses the conditional probability that a structural system reaches or exceeds a limit state when subjected to a specific ground motion intensity. In this paper, the fragility function is expressed as a log-normal cumulative distribution function, given by

$$P[\mathrm{LS}|\mathrm{IM}] = \Phi\left[\frac{ln(\mathrm{IM})-\mu}{\beta}\right] \quad (1)$$

where $P[\mathrm{LS}\,|\,\mathrm{IM}]$ is the probability of exceeding the limit state (LS) at a given ground motion intensity measure (IM). Here, IM is peak ground acceleration (PGA). Φ[-] is standard normal cumulative distribution function. μ and β are the median and standard deviation of $ln(IM)$, respectively. These two parameters were calculated using the maximum likelihood estimation (Shinozuka et al., 2000).

Figure 9 shows the fragility curves for three LSs and variation of LRB properties. It is apparently observed that the structural system performs without damage under earthquake with PGA less than 0.4g for

all the investigated cases. The change of elastic stiffness and yield strength of LRB gives a minor difference between fragility curves. Additionally, the curves are mostly identical for a variation of hardening ratio.

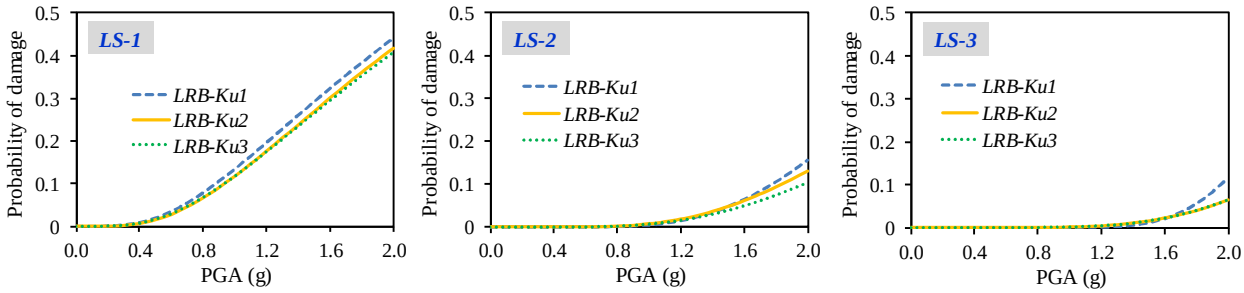

(a) various elastic stiffness

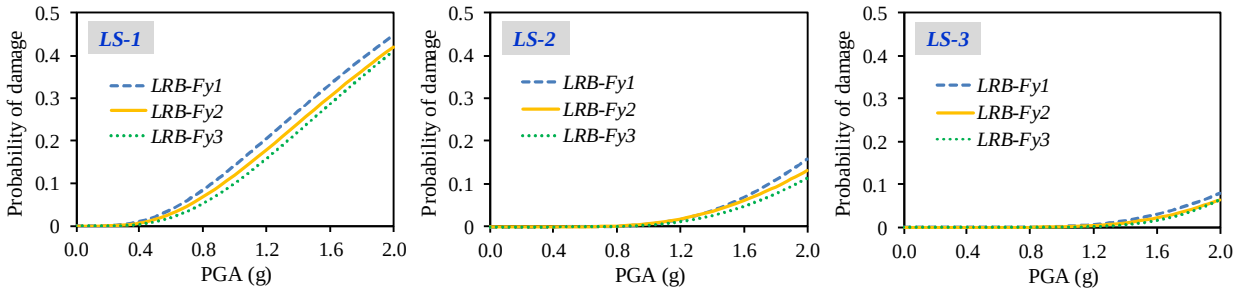

(b) various yield strength

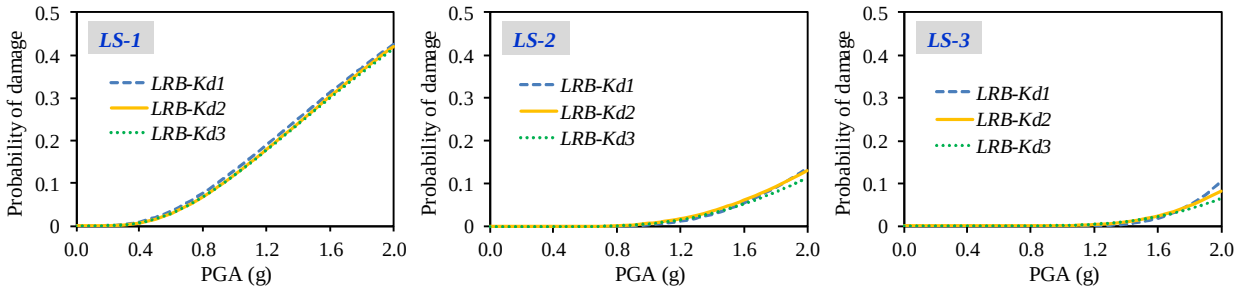

(c) various hardening ratio

Figure 9. Fragility curves of NPP for various properties of LRB

CONCLUSION

Seismic performances of a base-isolated NPP structure were evaluated based on a series of time-history analyses considering a variation of mechanical properties of LRB. FRS of containment building and shear deformation of LRB are obtained accounting a wide range of PGA. A set of fragility curves are developed for different limit states, which were defined in terms of the shear strain of LRB, using the maximum likelihood estimation. The influence of properties of LRB on FRS and fragility curves of NPP is examined. The following conclusions are drawn based on the numerical analysis results.

- FRS was significantly changed with a variation of the elastic stiffness of LRB. In contrast, the variation of the hardening ratio of LRB did not affect FRS of RCB.
- A variation of the yield strength of LRB moderately change FRS of RCB.
- For all three defined LSs, the effects of various properties of LRB on seismic fragility curves of the NPP are shown to be trivial.
- The base-isolated NPP structure performs without damage under motions with PGA less than 0.4g.

ACKNOWDLEGEMENT

This study is supported by projects entitled "*Development of high reliability seismic monitoring system for precise analysis of high frequency earthquake motion in nuclear power plants*" (number 20171510101860) and "*Analysis of seismic and fault characteristics for strengthening capacity for earthquake response of nuclear power plants and development of source technology for improving seismic performance*" (number 20171510101960).

REFERENCES

Ali, A., Hayah, N. A., Kim, D., & Cho, S. G. (2014). "Probabilistic seismic assessment of base-isolated NPPs subjected to strong ground motions of Tohoku earthquake," *Nuclear Engineering and Technology*, *46*(5), 699-706.

Cho, S. G., Yun, S. M., Kim, D., & Hoo, K. J. (2015). "Analyses of vertical seismic responses of Seismically isolated nuclear power plant structures supported by lead rubber bearings," *Journal of the Earthquake Engineering Society of Korea*, 19(3), 133-143.

Choun, Y. S., Park, J. & Choi, I. K. (2014). "Effects of mechanical property variability in lead rubber bearings on the response of seismic isolation system for different ground motions," *Nuclear Engineering and Technology*, 46(5), 605-618.

Eem, S. & Hahm, D. (2019). "Large strain nonlinear model of lead rubber bearings for beyond design basis earthquakes," *Nuclear Engineering and Technology*, 51(2), 600-606.

Hameed, A., Koo, M. S., Dai Do, T., & Jeong, J. H. (2008). "Effect of lead rubber bearing characteristics on the response of seismic-isolated bridges," *KSCE Journal of Civil Engineering*, 12(3), 187-196.

Jung, J. W., Jang, H. W., Kim J. H. & Hong, J. W. (2017). "Effect of second hardening on floor response spectrum of a base-isolated nuclear power plant," *Nuclear Engineering and Design*, 322, 138-147.

Kim, J. H., Kim, M. K. & Choi, I. K. (2016). "Experimental study on the ultimate limit state of a lead-rubber bearing," In *ASME 2016 Pressure Vessels and Piping Conference*, Vancouver, BC, Canada.

Kim, J-S., Jung, J-P., Moon, J-M., Lee, T-H., Kim, J-H. & Han, T-S. (2019). "Seismic fragility analysis of base-isolated LNG storage tank for selecting optimum friction material of friction pendulum system," *Journal of Earthquake and Tsunami*, DOI: https://doi.org/10.1142/S1793431119500106.

Lee, T. H., Choi, W. S., & Han, T. S. (2013). "Effect of base isolation on seismic fragility of aboveground LNG storage tanks," In *Proceedings of the Thirteenth East Asia-Pacific Conference on Structural Engineering and Construction (EASEC-13)*, Sapporo, Japan.

Lee, T-H. & Nguyen, D-D. (2018). "Seismic vulnerability assessment of a continuous steel box girder bridge considering influence of LRB properties," *Sadhana*, 43, 14.

Lee, J. H., & Song, J. K. (2015). "Comparison of seismic responses of seismically isolated NPP containment structures using equivalent linear-and nonlinear-lead-rubber bearing modelling," *Journal of the Earthquake Engineering Society of Korea*, *19*(1), 1-11.

Nguyen, D-D., Thusa B. & Lee, T-H. (2018). "Seismic fragility of base-isolated nuclear power plant considering near-fault ground motions," *Journal of the Korean Society of Hazard Mitigation*, 18(7), 315-321.

Nguyen, D-D., Thusa B. & Lee, T-H. (2019). "Effects of significant duration of ground motions on seismic responses of base-isolated nuclear power plant," *Journal of the Earthquake Engineering Society of Korea*, 23(3), 149-157.

Park, H-S., Nguyen, D-D. & Lee, T-H. (2017). "Effect of high-frequency ground motions on the response of NPP components: A state-of-the-art review," *Journal of the Korean Society of Hazard Mitigation*, 17(6), 285-294.

Providakis, C. P. (2008). "Effect of LRB isolators and supplemental viscous dampers on seismic isolated buildings under near-fault excitations," *Engineering Structures*, 30(5), 1187-1198.

Shinozuka M., Feng, M. Q., Lee, J. & Nagamuma T. (2000). "Statistical analysis of fragility curves," *Journal of Engineering Mechanics*, ASCE, 126(12), 1224-1231.

Xie, W-C., Jiang W., Ni S-H., & Liu W. (2019). *Seismic risk analysis of nuclear power plants*, Cambridge University Press.

Yabana, S., Kanazawa, K., Nagata, S., Kitamura, S., & Sano, T. (2009). "Shaking table tests with large test specimens of seismically isolated FBR plants: Part 3 - Ultimate behaviour of upper structure and rubber bearings," In *ASME 2009 Pressure Vessels and Piping Conference*, Prague, Czech Republic.

Zhang, J., & Huo, Y. (2008). "Optimum isolation design for highway bridges using fragility function method," In *The 14th World Conference on Earthquake Engineering (WCEE)*, Beijing, China.